E13-2001-113

A.Yu.Petrus, B.Zh.Zalikhanov

ELECTRO-MECHANICAL PROPERTIES OF NARROW-GAP MULTIWIRE PROPORTIONAL CHAMBERS

Submitted to «Nuclear Instruments and Methods in Physics Research, Section A»

1 Introduction

Narrow-gap multiwire proportional chambers were first suggested as detectors for electromagnetic calorimeters in Ref. [1]. In this paper considerable attention was given to investigation of the amplitude characteristics, which is of crucial importance for the calorimetric measurements. Coordinate detectors with a spatial resolution of $\sim$1 mm and that can operate in the high rate environment were studied in Ref. [2]. Moreover, in this paper the use of a gas mixture of CF_4 with hydrocarbons was suggested. This made it possible to obtain a very narrow time jitter together with a high registration efficiency for minimum ionizing particles. Somewhat later [3, 4] it was shown that the gas mixture with CF_4 slows down the ageing of the chamber, which is very important when chambers are operated in a high rate environment. Nevertheless, it should be noted that the use of such chambers in experiments comes across considerable difficulties associated with the formation of induced discharges as well as with wire instabilities.

Such chambers were first used in an experimental study of rare K-meson decays at the ISTRA setup as beam chambers [5]. Because of the new frameless technology of construction and special measures to provide precision of the wire positioning [6], it was possible to achieve a stable performance of the chamber with a sensitive area of 140×130 mm^2. At the same time, the plateau was 1400 V and the achieved coordinate resolution amounted to 320 μm (r.m.s). These chambers showed stable performance during a long period of time without any noticeable deterioration of the characteristics despite high counting rates. Similar chambers with a sensitive area several times larger are also used as coordinate detectors of the forward spectrometer at the ANKE setup working on the internal beam of the COSY synchrotron [7].

New experiments aimed at investigating rare processes as well as experiments being conducted and planned on internal beams impose heavy demands on the employed track detectors. In particular, proportional chambers must show stable performance for an appreciable length of time in the high rate environment, have small dead time, contain small amount of material along the path of the registered particles, at the same time provid a high registration efficiency and cover considerable areas ($\gtrsim$1000 cm^2).

This situation demands a more thorough investigation of the electro-mechanical properties of narrow-gap chambers. It should be noted that such chambers have a number of important distinctive features in comparison with the usual chambers with the gap $\sim$5–10 mm. A small gap leads to an increase in the capacity of the wire, which makes it necessary to work at higher voltages as accounted for by the unit of the gap length. This leads to an increased wire displacements from the central position and, as a result, to a higher probability of breakdown by spark development in the anode-cathode gap. In order to avoid this, the wire tension has to be increased, which, in turn, imposes a limitation on the tolerable length of the wires. Apart from this, as is seen from what is given bellow, various inaccuracies in the construction have much large influence on the characteristics of narrow-gap

chambers as compared to the characteristics of standard chambers.

The electric field potential in the multiwire proportional chamber (Fig.1) can be found by the method of images using the complex potential theory [8, 9]. As described in Ref. [9], for a symmetrical chamber (when the wires are centrally located between the cathode planes) on the assumption that the wire radius r_0 is very small in comparison with the distance between the wires s, one can obtain a simple equation for the electric field in the chamber:

$$|E| = \frac{U_0}{2|\tan(\pi\zeta/s)|\epsilon_0(\pi\zeta/s - 2\ln(2\pi r_0/s))}, \tag{1}$$

where $\zeta = x + iz$. Unfortunately, this formula does not allow consideration of effects connected with the wire displacement in the chambers, as it is applicable only to the symmetric case.

In Ref. [10] an equation for the electric field potential was obtained in the form of a sum over the wires, which allowed consideration of the effects connected with the displacement of a separate wire in the chamber. This made it possible to achieve certain limitations on possible inaccuracies in the construction of standard chambers.

The aim of this work is i) to study the electro-mechanical properties of multiwire narrow-gap proportional chambers; ii) investigate the stability of wires depending on different parameters of the chamber; iii) study the influence of the inaccuracies in construction of the chamber on the chamber's operating characteristics.

2 Electric field of the multiwire proportional chamber

The calculation of the field strength by the method of images is possible to base directly on the equations for the strength of the field produced by each charge, when not the potentials but the field strengths are summed. This approach, equivalent to that developed in Ref. [8] and applied in [10] for the case when the wire presents a direct line, is much more convenient (in comparison with the summation over the potentials) in calculating the fields when the wires do not form stright lines.

Let us consider a multiwire proportional chamber with the standard geometry as depicted in Fig. 1. Let the linear density of the charge on the wire be equal to η. The electric field strength of the linear charge is equal to

$$E = \frac{\eta}{2\pi\epsilon_0 r}, \tag{2}$$

or in the projections:

$$E_x = \frac{\eta x}{2\pi\epsilon_0 r^2}, \quad E_z = \frac{\eta z}{2\pi\epsilon_0 r^2} \tag{3}$$

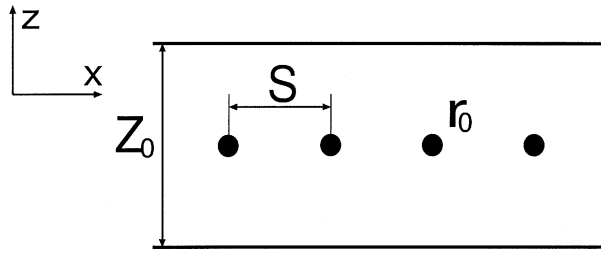

Figure 1: Configuration of a standard proportional chamber.

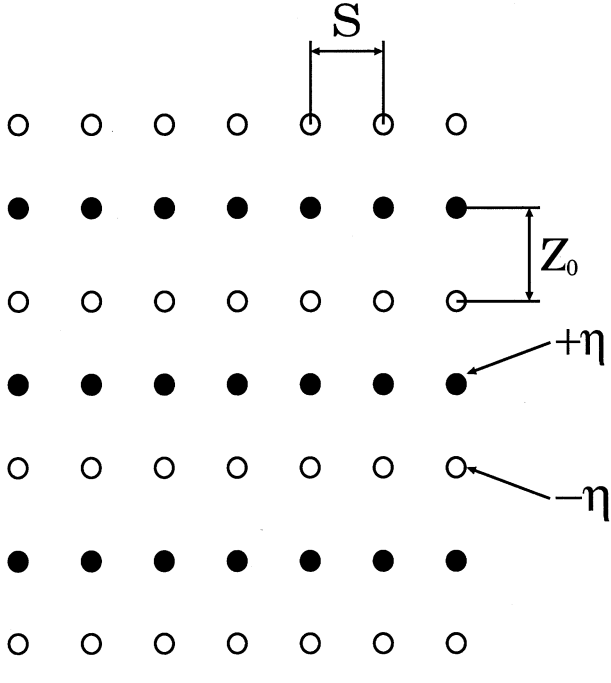

Figure 2: Configuration of charges and their reflections for which the field is calculated.

When the method of images is employed, the task reduces to the calculation of the electric fields of the charges located in the sites of the rectangular lattice (Fig. 2), as each wire placed between conducting planes causes an infinite number of reflections of the alternating signs. In what follows the reflections of the wires in each other are disregarded, that is it is assumed that the diameter of the wire is much less than the distance between the wires.

Let the central wire of the chamber be located at a point with the coordinates $x = z = 0$. Then, the equation for the electric field in the chamber will have the form of a double sum, where each component represents the field produced by the corresponding charge at the point (x, z).

$$\begin{aligned} E_x &= \frac{\eta}{2\pi\epsilon_0} \sum_{k=-m}^{m} \sum_{n=-\infty}^{\infty} \frac{(-1)^n (x - ks)}{(x - ks)^2 + (z - nz_0)^2}, \\ E_z &= \frac{\eta}{2\pi\epsilon_0} \sum_{k=-m}^{m} \sum_{n=-\infty}^{\infty} \frac{(-1)^n (z - nz_0)}{(x - ks)^2 + (z - nz_0)^2}, \end{aligned} \tag{4}$$

where $2m + 1$ is the number of the wires in the chamber.

As was indicated in Ref. [10], two orders of summing these series are possible: first they are summed over the number of the image, then over the number of the wire, and vice versa. But if the aim is to study the changes in the field in the chamber, which are connected with the displacements of separate signal wires in the chamber, the first order of summing the series should be chosen as the most suitable one. In this case for the components of the electric field the following equations are obtained

$$\begin{aligned} E_x &= \frac{\eta}{\epsilon_0 z_0} \sum_{k=-m}^{m} \frac{\sinh[\pi(x - ks)/z_0] \cos \pi z/z_0}{\cosh[2\pi(x - ks)/z_0] - \cos 2\pi z/z_0}, \\ E_z &= \frac{\eta}{\epsilon_0 z_0} \sum_{k=-m}^{m} \frac{\cosh[\pi(x - ks)/z_0] \sin \pi z/z_0}{\cosh[2\pi(x - ks)/z_0] - \cos 2\pi z/z_0}. \end{aligned} \tag{5}$$

Now it is necessary to express the unknown linear density of the charge on the wire in terms of the value of the potential at the cathode of the chamber. Let the potential at the cathode be equal to U_0, the potential of a wire with the radius r_0 be equal to 0. On the line connecting the wire with one of the cathodes and parallel to the axis Z, $E_x = 0$. Then the condition connecting the linear density of the charge η with the potential of the cathode will take the following form

$$-U_0 = \int_{r_0}^{z_0/2} E_z(x=0,z)dz = \frac{\eta}{\epsilon_0 z_0}\int_{r_0}^{z_0/2}\sum_{k=-m}^{m}\frac{\cosh[\pi(x-ks)/z_0]\sin\pi z/z_0}{\cosh[2\pi(x-ks)/z_0]-\cos 2\pi z/z_0}dz. \tag{6}$$

Calculating the integral on the right of eq. (6) (see Ref. [11]) for the linear density of the charge, we obtain

$$\eta = 2\pi\epsilon_0 U_0 \Big/ \sum_{k=-m}^{m}\operatorname{arctanh}\left[\frac{\cos\pi r_0/z_0}{\cosh\pi ks/z_0}\right]. \tag{7}$$

Now for the components of the electric field, we obtain:

$$E_x = \frac{2\pi U_0}{z_0 C_0}\sum_{k=-m}^{m}\frac{\sinh[\pi(x-ks)/z_0]\cos\pi z/z_0}{\cosh[2\pi(x-ks)/z_0]-\cos 2\pi z/z_0},$$
$$E_z = \frac{2\pi U_0}{z_0 C_0}\sum_{k=-m}^{m}\frac{\cosh[\pi(x-ks)/z_0]\sin\pi z/z_0}{\cosh[2\pi(x-ks)/z_0]-\cos 2\pi z/z_0}, \tag{8}$$

where

$$C_0 = \sum_{k=-m}^{m}\operatorname{atanh}\left[\frac{\cos\pi r_0/z_0}{\cosh\pi ks/z_0}\right]. \tag{9}$$

It should be noted that the value $2\pi\epsilon_0/C_0$ represents the capacity of the wire.

Formulas (8) and (9) allow one to compare the distributions of the electric field as well as the corresponding geometry of avalanche formation areas in standard and narrow-gap chambers. With this purpose let us consider the following characteristic configurations of the electrodes:

1. $z_0/2 = 8$ mm, $s = 2$ mm, $r_0 = 10$ μm;
2. $z_0/2 = 1.5$ mm, $s = 1$ mm, $r_0 = 10$ μm;
3. $z_0/2 = 2$ mm, $s = 2$ mm, $r_0 = 10$ μm.

From here on these configurations will be referred to as "chamber 1", "chamber 2" and "chamber 3".

The electric field distribution along the line with $x = 0$ is shown in Fig. 3,a and Fig. 4,a. The calculations have shown that the given value E/p averaged over the drift path for narrow-gap chambers 2 and 3 is larger than in the standard chamber 1 factor 5 to 8. If at atmospheric pressure the value of the field is taken to be 20kV/cm as the threshold value of avalanche formation in the mixtures CF_4 and

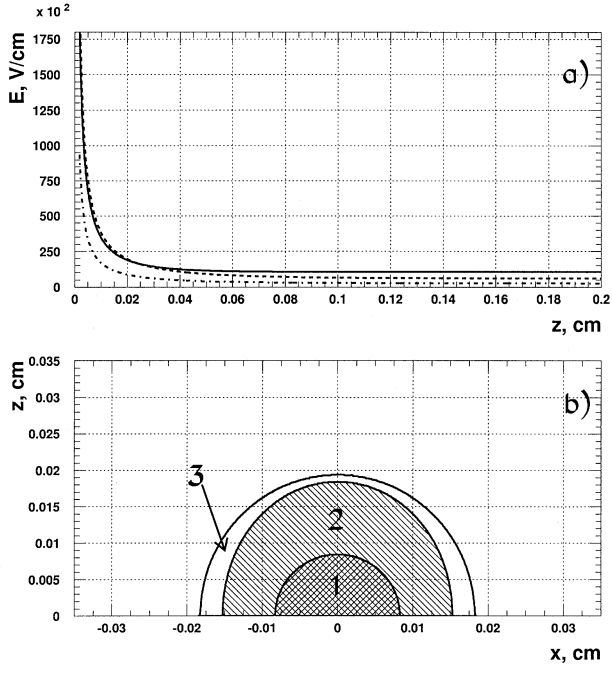

Figure 3: **a)** Avalanche formation region near the anode wire limited by the value of field strength 20 kV/cm for three different chambers (see explanation in the text); **b)** electric field distribution in the direction to the cathode: (-.-.-) - chamber 1; (—) - chamber 2; (- - -) - chamber 3. The chamber voltage is 2500 V.

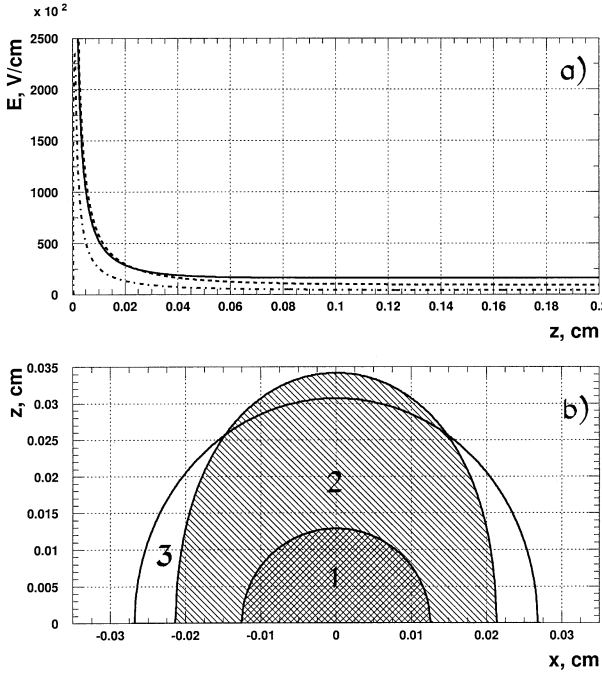

Figure 4: The same as in Fig.3, the chamber voltage is 3800 V.

iso-C_4H_{10} (this conclusion can be made based on the dependence of the Townsend first coefficient α on the field intensity [13]), at the chamber's voltage 3.8 kV this field will be produced at a distance of 0.35 mm from the anode wire for chamber 2, at the distance of 0.3 mm for chamber 3 and only at 0.12 mm for chamber 1. The corresponding form of the avalanche formation areas are shown in Fig. 3,b and Fig. 4,b. It is evident that the avalanche formation areas in narrow-gap chambers are substantially larger than the corresponding areas in the standard chamber.

3 Equilibrium configuration of the wires in a proportional chamber

Problems connected with the stability of the wire configuration at given parameters of the chamber (voltage, wire tension, etc.) are of no little importance, as their solution allows one to optimize the construction, to determine the minimal necessary wire tension.

In the chamber depicted in Fig. 1 charges of the same sign are induced on the wires, with repulsive forces between them. Even when all geometrical characteristics are absolutely precisely given in the construction of the chamber, the equilibrium configuration of the wires will be different from the ideal configuration depicted in Fig. 1. The wires will tend to shift from the center of the gap and will achieve an equilibrium configuration when the electrostatic repulsion force is compensated by the elastic deformation of the strained wire. At the same time the form of the wire will be described by a function $z = f(y)$, where y is the coordinate along the wire.

For the determination of the equilibrium configuration of wires a method analogous to the one described in Ref.[12] can be employed. This method consists in minimization of the functional of the potential energy of the wires in the electrostatic field. Unlike in Ref. [12], where the equilibrium form of the wire in a drift tube was considered, the contribution of gravitational forces can be disregarded in the case of multiwire chambers, as wires in proportional chambers are much thinner (which means that they have a much less weight) and much shorter in comparison with the wires in drift tubes. Thus, the wire potential energy will include two terms

$$PE = PE_T + PE_E, \tag{10}$$

where PE_T is the energy of the wire elastic deformation (extension), PE_E is the electrostatic energy of the charge induced on the wire.

From symmetry considerations it is seen that all wires fall into two groups. And if for one group of wires (let us call them "even") the form is described by the function $z = f(y)$, for the other group of wires ("odd") it is described by the function $z = -f(y)$. It is also evident that $f(y)$ has to be an even function of the variable y. Apart from this, there is no necessity to sum the energy of all the wires of

the chamber. It is enough to consider only one wire and the chamber cell connected with it.

Let us consider the electrostatic part of the functional. Let $\eta(t)$ be the linear charge density induced on the wire. Then the charge of the infinitesimal part of the wire dl at the point $x', y' = t$, $z' = f(t)$ produces the field at the point x, y, z inside the chamber:

$$\begin{aligned} dE_x &= \frac{\eta(t)dl}{4\pi\epsilon_0} \sum_{n=-\infty}^{\infty} \frac{(-1)^n(x-x')}{[(x-x')^2+(y-t)^2+(z-nz_0-(-1)^n f(t))^2]^{3/2}}, \\ dE_y &= \frac{\eta(t)dl}{4\pi\epsilon_0} \sum_{n=-\infty}^{\infty} \frac{(-1)^n(x-x')}{[(y-y)^2+(y-t)^2+(z-nz_0-(-1)^n f(t))^2]^{3/2}}, \\ dE_z &= \frac{\eta(t)dl}{4\pi\epsilon_0} \sum_{n=-\infty}^{\infty} \frac{(-1)^n(z-nz_0-(-1)^n f(t))}{[(x-x')^2+(y-t)^2+(z-nz_0-(-1)^n f(t))^2]^{3/2}}. \end{aligned} \tag{11}$$

Summing over n takes into consideration the field produced not only by the wire but also by its images. In order to find the total field produced by all the wires, except for the considered one, it is necessary to integrate over l and to sum over all the wires, except for the case $n = k = 0$. It is easy to see that

$$dl = \sqrt{1+[f'(t)]^2}dt. \tag{12}$$

Then

$$E_x = \frac{1}{4\pi\epsilon_0} \sum_{k=-m}^{m} \sum_{n=-\infty}^{\infty} \int_{-L/2}^{L/2} \frac{(-1)^n(x-x')\eta(t)\sqrt{1+[f'(t)]^2}dt}{[(x-x')^2+(y-t)^2+(z-nz_0-(-1)^{n+k}f(t))^2]^{3/2}}, \tag{13}$$

where the term with $n = k = 0$ is excluded from summation. Analogous expressions can be obtained for E_y and E_z. The electrostatic part of the potential energy is given by the expression

$$PE_E = \int_{-L/2}^{L/2} \eta(y)\sqrt{1+[f'(y)]^2} \int_{z_b(y)}^{z_0/2} E_z(x=0,y,z)dzdy, \tag{14}$$

where $z_b(y) = f(y) + r_0$.

Clearly the minimization of such a functional with respect to the two functions $\eta(y)$ and $f(y)$ is a difficult to realize. That is why it is necessary to make additional assumptions simplifying the solution of the problem. From here on let us assume that $\eta(t) = \eta \equiv const$ and that the wire form is described by a parabola:

$$f(t) = at^2 + bt + c. \tag{15}$$

According to the conditions of the task, the function $f(t)$ must satisfy the boundary conditions $f(L/2) = f(-L/2) = 0$. This allows one to reduce $f(t)$ to the form

$$f(t) = at^2 - aL^2/4. \tag{16}$$

It is easy to see that a is related to z_{max}, the maximum displacement of the wire from the center of the gap, $z_{max} = -aL^2/4$. Thus, there is only one free parameter a left, with respect to which it is necessary to minimize the functional of the potential energy.

Taking into account the above mentioned allowances, the electrostatic part of the functional can be presented in the following form:

$$PE_E = \frac{\eta^2}{4\pi\epsilon_0} \sum_{k=-m}^{m} \sum_{n=-\infty}^{\infty} \int_{-L/2}^{L/2} \int_{-L/2}^{L/2} \int_{z_b(y)}^{z_0/2} \frac{(-1)^n (z - nz_0 - (-1)^{n+k}(at^2 - aL^2/4))\sqrt{1+4a^2t^2}\sqrt{1+4a^2y^2}}{[(ks)^2 + (y-t)^2 + (z - nz_0 - (-1)^{n+k}(at^2 - aL^2/4))^2]^{3/2}} dz dt dy, \tag{17}$$

where $z_b(y) = ay^2 - aL^2/4 + r_0$ and the term is excluded from the summation with $k = n = 0$.

For the calculation of η a formula analogous to eq. (6) can be employed:

$$-U_0 = \int_{z_b(0)}^{z_0/2} E_z(x = 0, y = 0, z) dz. \tag{18}$$

As is known, the energy of elastic deformation of the wire is determined by the expression

$$\begin{aligned} PE_T =& T_0 \int_{-L/2}^{L/2} \sqrt{1 + [f'(t)]^2} dt - T_0 L = T_0 \int_{-L/2}^{L/2} \sqrt{1 + 4a^2t^2} dt - T_0 L = \\ & T_0 \Big(\frac{L\sqrt{1+a^2L^2}}{2} + \frac{1}{4a} \ln \Big[\frac{aL + \sqrt{1+a^2L^2}}{-aL + \sqrt{1+a^2L^2}} \Big] - L \Big). \end{aligned} \tag{19}$$

The integration over z in the expression for PE_E is can be carried out analytically. The other two integration over t and over y was calculated numerically.

The results of the calculation of the dependence of the functional of the wire potential energy on the displacement of z_{max} are shown in Fig. 5 for two cases. In the first case (Fig.5.a) the minimum is observed at $z_{max} \simeq 0.085$ mm, which testifies to the stability of the wire in the chamber with the geometrical parameters indicated in the Fig. 5.a In the case of higher voltage applied to the chamber (Fig. 5.b), a minimum of the potential energy of the wire is not observed and that means that wire will be unstable.

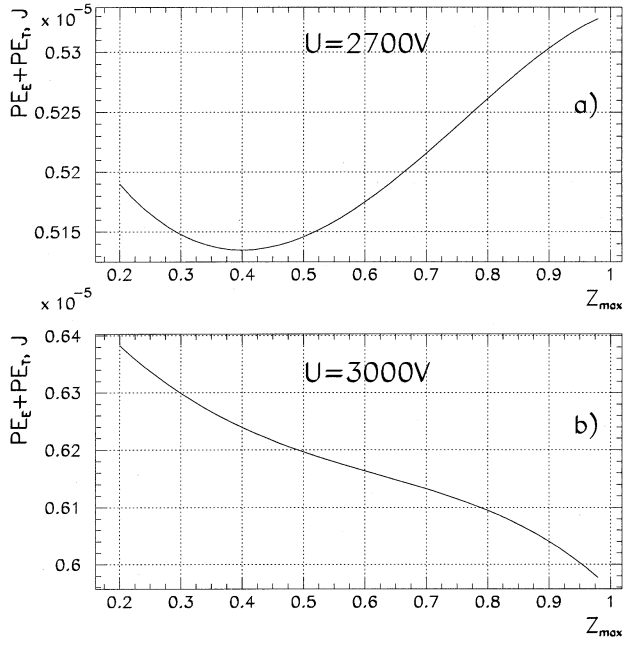

Figure 5: The potential energy of the wire as a function of the value of the wire maximum displacement from the center of the gap z_{max} for the chamber with $z0/2 = 2.0mm$, $s = 2.0$ mm, $T_0 = 0.5$ N, $r_0 = 10$ μn, $L = 50$ cm: a) stable configuration at the cathode voltage $U = 2700$ V; b) unstable configuration at the voltage $U = 3000$ V.

In Fig. 6 the limits of the wire stability are illustrated for different chambers. It is necessary to note that a given results refer only to the mechanical stability of the wires and not to the stability with respect to electric discharges between wires and cathode. Thus, for example, the wires in the chamber with $s = 1.0$ mm and $z_0/2 = 1.5$ mm will be mechanically stable at the chamber's length $L = 25$ cm and voltage $U = 6000$ V, but at this voltage an electric discharge between the wire and the cathode is bound to arise. As far as the chambers with a large gap ($z_0/2 > 5$ mm) are concerned, the wires are mechanically stable in a very wide voltage range (certainly providing sufficient amplification) as well as in a wide length range exceeding $1.5 - 2$ m. It should be noted that for wires of such a length gravitational forces will play an important role, except when the wires are oriented vertically.

4 Influence of the spatial shift of the wires on the value of gas amplification in the chamber

One of the most important characteristics of a chamber is the homogeneity of gas amplification, that is its independence of the primary electron cluster formation. The formulas presented above allow calculation of the field at any point of the chamber as well as, given the dependence of the Townsend first coefficient α on the electric field strength, an evaluation of the dependence of the amplification on the maximum displacement of the wire z_{max}.

For the evaluation of gas amplification the data for α for CF_4 given in Ref. [13] were used. The amplification was calculated according to the formula

$$G = \exp(\int \alpha(E)dl), \tag{20}$$

where integration was carried out along the electron path of motion. This formula does not take into account the influence of the avalanche space charge, which becomes noticeable at large amplification ($\gtrsim 10^5$), as well as the influence of the avalanche diffusion and the statistic character of the cluster formation along the particle trajectory. Nevertheless, this formula is suitable for calculations if it is considered as an approximation which allows evaluation of the effect of different factors on the amplification in the chamber.

In Fig. 7.a the dependence of the linear charge density as a function of the wire displacement from the cathode is shown. The change of the charge density also leads to the change of amplification near the wire [10]. But apart from this, the amplification is also influenced by the change in the electron motion path at the wire displacement. In Fig. 7.b and Fig. 7.c the gas amplification as a function of the wire displacement is depicted, the condition being that the primary electron is produced in the immediate vicinity of the cathode. Also it should be taken into

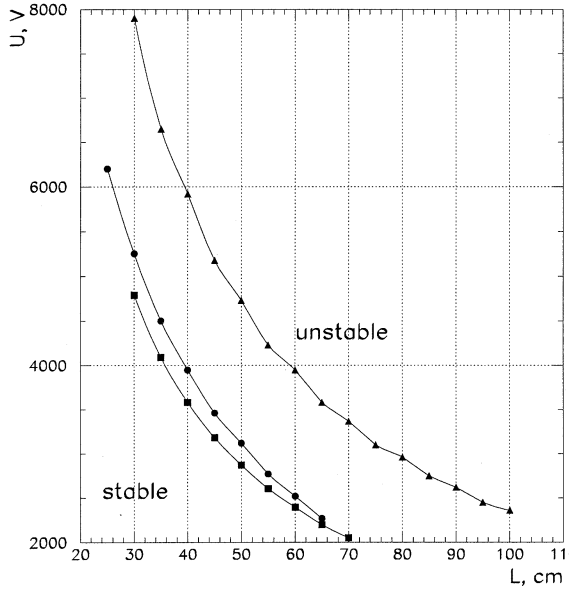

Figure 6: The wire stability area limits for different chambers. The chamber parameters are:
• — $z_0/2 = 1.5$ mm, $s = 1.0mm$, $T_0 = 0.5N$, $r_0 = 10$ μm;
■ — $z_0/2 = 2.0$ mm, $s = 2.0$ mm, $T_0 = 0.5$ N, $r_0 = 10$ μm;
▲ — $z_0/2 = 3.0$ mm, $s = 2.5$ mm, $T_0 = 0.5$ N, $r_0 = 12.5$ μm.

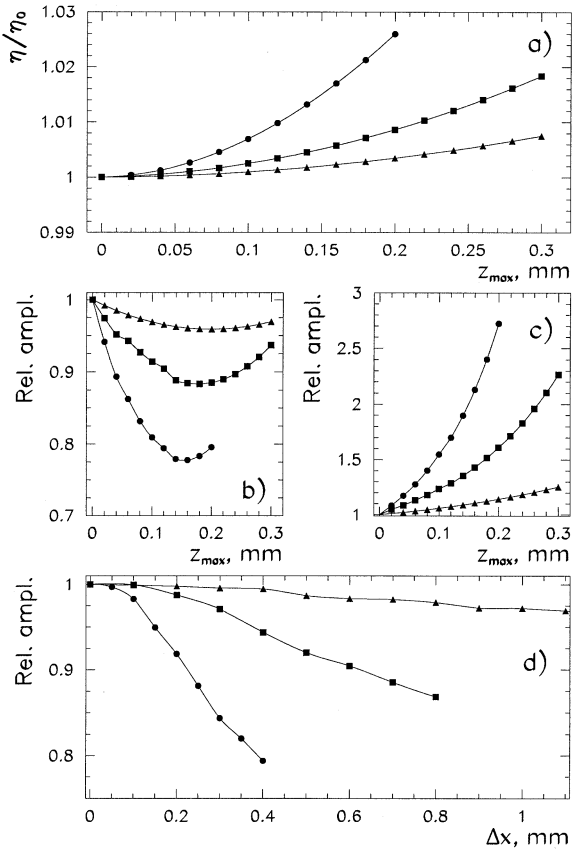

Figure 7: a) The linear charge density of a wire normalized to the density of the charge of the non-displaced wire as a function of the wire displacement; b) Relative amplification, with the primary electron starting its motion at the cathode from which the wire is displaced by z_{max}; c) Relative amplification with the primary electron starting its motion at the cathode to which the wire is moved by z_{max}; d) Relative amplification with the primary electron starting its motion at the cathode depending on the horizontal coordinate Δx (the coordinate of the wire corresponds to $\Delta x = 0$). The parameters of the chambers are:
• — $z_0/2 = 1.5$ mm, $s = 1.0$ mm, $T_0 = 0.5$ N, $r_0 = 10$ μm, $L = 20$ cm, $U_0 = 2500$ V;
■ — $z_0/2 = 2.0$ mm, $s = 2.0$ mm, $T_0 = 0.5$ N, $r_0 = 10$ μm, $L = 30$ cm, $U_0 = 3000$ V;
▲ — $z_0/2 = 5.0$ mm, $s = 2.0$ mm, $T_0 = 0.5$ N, $r_0 = 12.5$ μm, $L = 70$ cm, $U_0 = 3000$ V.

consideration that in Fig. 7.b this dependence is shown for the case when the wire is displaced in the direction from the cathode near which the electron was produced. At small displacements the amplification decreases despite the growthing the wire charge density, as the field is reduced on the side of the wire due to its removal from the cathode. But as the displacement is further increased, the influence of the charge density growth starts to prevail over the displacement from the cathode, and the amplification begins to increase. In the case of the wire displacement in the direction of the cathode, near which the electron is produced (Fig 7.c), both factors work together; as the displacement growths, the amplification increases with much more intensity in comparison with the opposite case.

The value of gas amplification is affected by the location of the primary electron production. In Fig.7.d dependence of the gas amplification as a function of primary electron position is shown (it is assumed again that the electron is produced near the cathode). It should be noted that the maximum amplification is achieved when the primary electron is produced at the x-coordinate of the wire itself, the minimum amplification is achived when the production takes place near the center between the wires.

Let us consider the case when one of the wires (let us call it "wire 0") is displaced in the direction parallel to the cathode. For the field calculations the method analogous to the one described in Sect. 2 can be used in this case. Instead of eqs. (5) for the electrostatistic field we obtain

$$\begin{aligned} E_x &= \frac{1}{\epsilon_0 z_0}\left[\sum_{\substack{k=-m \\ k\neq 0}}^{m} \eta_k \frac{\sinh[\pi(x-ks)/z_0]\cos\pi z/z_0}{\cosh[2\pi(x-ks)/z_0]-\cos 2\pi z/z_0} + \right. \\ &\qquad \left. \eta_0 \frac{\sinh[\pi(x-\Delta x)/z_0]\cos\pi z/z_0}{\cosh[2\pi(x-\Delta x)/z_0}\right], \\ E_z &= \frac{1}{\epsilon_0 z_0}\left[\sum_{\substack{k=-m \\ k\neq 0}}^{m} \eta_k \frac{\cosh[\pi(x-ks)/z_0]\sin\pi z/z_0}{\cosh[2\pi(x-ks)/z_0]-\cos 2\pi z/z_0} + \right. \\ &\qquad \left. \eta_0 \frac{\cosh[\pi(x-\Delta x)/z_0]\sin\pi z/z_0}{\cosh[2\pi(x-\Delta x)/z_0}\right], \end{aligned} \tag{21}$$

where η_0 and η_k are the linear densities of the charges of displaced and non-displaced wires, correspondingly.

In order to find $2m+1$ charge densities, let us use $2m+1$ conditions analogous to Eq. (6):

$$-U_0 = \int_{r_0}^{z_0/2} E_z(x=\Delta x, z)dz; \; -U_0 = \int_{r_0}^{z_0/2} E_z(x=ks, z)dz, \; -m \leq k \leq m, \; k \neq 0. \tag{22}$$

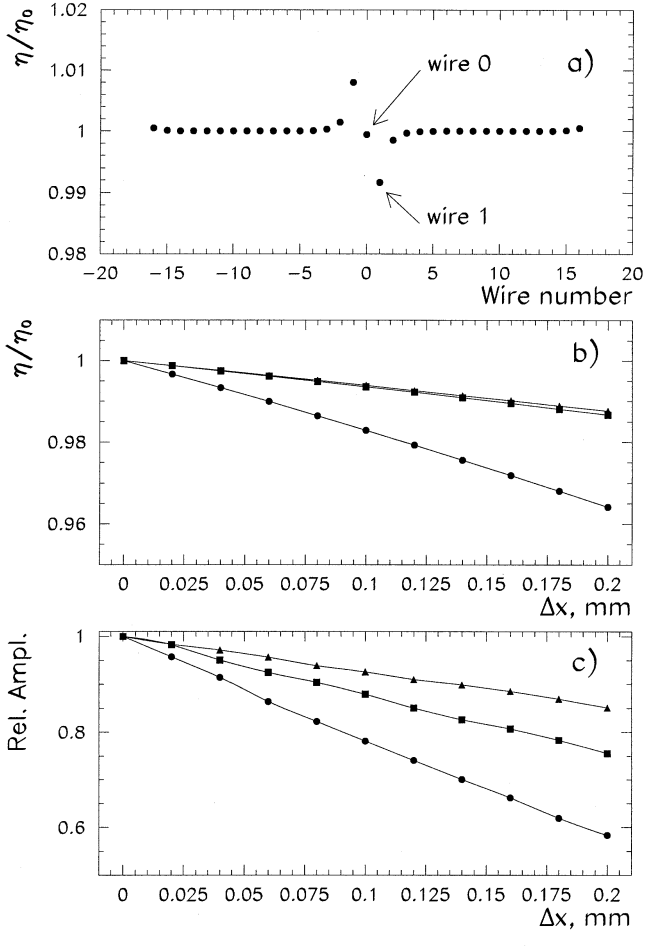

Figure 8: a) Relative linear induced charge density as a function of the sign of the wire, provided that the wire with the number 0 is displaced by $\Delta x = 50$ μm in the direction towards the wire with the number 0 (η_0 is the density of the charge of the wire far away from the displaced one); b) Relative linear induced charge density on the wire with the number 1 depending on the value of the wire 0 displacement; c) Relative amplification of wire 1 at the wire 0 displacement. The parameters of the chambers are the same as in Fig. 7.

Making use of these conditions we obtain a system of $2m+1$ linear equations with $2m+1$ unknowns η_k:

$$2\pi\epsilon_0 U_0 = \sum_{\substack{k=-m \\ k\neq 0}}^{m} \eta_k \operatorname{atanh}\left[\frac{\cos \pi r_0/z_0}{\cosh(\pi(\Delta x - ks)/z_0)}\right] + \eta_0 \operatorname{atanh}(\cos\frac{\pi r_0}{z_0}),$$

$$2\pi\epsilon_0 U_0 = \sum_{\substack{k=-m \\ k\neq 0}}^{m} \eta_k \operatorname{atanh}\left[\frac{\cos \pi r_0/z_0}{\cosh(\pi(l-k)s/z_0)}\right] + \eta_0 \operatorname{atanh}\left[\frac{\cos \pi r_0/z_0}{\cosh(\pi(ls - \Delta x)/z_0)}\right], \tag{23}$$

where $m \leq l \leq m$, $l \neq 0$. Solving this system for η_k, it is possible to find the charge densities on all wires, which means to calculate the electrostatic field.

In Fig. 8.a the relative change in the charge densities at the wire 0 displacement by $\Delta x = 50$ μm is shown. As is seen from the Fig. 8.a, this displacement makes the maximum influence not on the charge density of the displaced wire but on the charge density of the neibouring wires. The charge density of wire 1 as a function of the displacement of wire 0 is illustrated in Fig. 8.b. The amplification of wire 1 as a function of the displacement of wire 0 is depicted in Fig. 8.c.

As could be expected, the density of the charge induced on the wire as well as the gas amplification in the chamber with a smaller spacing between the wires and a smaller gap between the wires and the cathode turns out to be more sensitive to a change of the wire position compared to a chamber with a larger spacing and a large gap. This in turn imposes more rigid limitations on the precision of construction of narrow-gap proportional chambers. For example, if we restrict ourself by the requirement that the amplification range in the chamber should not exceed $\pm 25\%$, the maximum acceptable length of the wire in the chamber with $z_0/2 = 1.5$ mm, $s = 1.0$ mm will be about $25 - 30$ cm, which is $35 - 40$ cm for a chamber with $z_0/2 = 2.0$ mm, $s = 2.0$ mm, whereas for a chamber with $z_0/2 = 5.0$ mm, $s = 2.5$ mm it amounts to $90-100$ cm. As far as the compliance with the wire spacing uniformity is concerned, with the same assumptions the permissible inaccuracy amounts to $\Delta x \simeq 85$ μm, $\Delta x \simeq 175$ μm, $\Delta x \simeq 250\mu$ m for the three chambers discussed above, correspondingly.

5 Conclusion

In the paper it was shown that unlike chambers with a large gap, limitations connected with the mechanical stability of wires are of importance for narrow-gap chambers. An equation which allows one to evaluate the wire stability limits is obtained. The influence of the wire displacement on the amplitude characteristics of the chamber is considered. It is important to note that the results on the amplitude characteristics are of the evaluative character. In order to account for various processes taking place

in the chamber, it is necessary to proceed from a realistic model taking into account the statistical character of the avalanche formation as well as various characteristics of the gas discharge. At present we are developing a model based on Monte-Carlo calculations taking into account electron-molecular cross-sections. This model will allow us gain futher insight into the processes of the formation and development of electron avalanches in gases.

6 Acknowledgements

We would like to acknowledge the hospitality of Forschungszentrum Jülich (Germany) where a part of this work was carried out. The authors are grateful to Prof. V.I.Komarov, Dr. F.Rathmann and Dr. H.Seyfarth for a careful reading of the manuscript and valuable comments. Special thanks are to the Irish Pub "Linch's", in particular to Ross and Bob for creating a warm and crazy atmosphere.

References

[1] S.Majewski et al, **NIM 217 (1983) 265.**

[2] J.Fischer et al, **NIM A238 (1985) 249.**

[3] R.Handerson et al, **IEEE Trans. Nucl. Sci, NS-34 (1987) 528.**

[4] R.Handerson et al, **IEEE Trans. Nucl. Sci, NS-35 (1988) 477.**

[5] E.M.Gushcin et al, **NIM A351 (1994) 345.**

[6] H.Kalmar et al., **NIM A307 (1991) 279.**

[7] O.W.B.Schult et al., **Nucl.Phys. A583 (1995) 629.**

[8] P.M.Morse and H.Feshbach, "Methods of thepretical physics", Part 2, (New York, 1953), p1241.

[9] G.A.Erskine, **NIM 105 (1972) 565.**

[10] G.V.Alexeev et al., **P13-10606, (1977), JINR** (in Russian).

[11] A.P.Prudnikov, Yu.A.Brychkov, O.I.Marichev, "Integrals and Series" (in Russian), (Moskow, 1981).

[12] R.H.Milburn, **NIM A394 (1997) 415.**

[13] L.G.Christophorou and J.K.Olthoff, **J.Phys.Chem.Ref.Data, 28 (1999) 967.**

Received by Publishing Department
on May 30, 2001.

Петрус А.Ю., Залиханов Б.Ж. E13-2001-113
Электромеханические свойства
узкозазорных многопроволочных пропорциональных камер

Рассмотрены электромеханические свойства узкозазорных пропорциональных камер. Получено соотношение, позволяющее оценить пределы рабочей области по напряжению в зависимости от геометрических характеристик камеры. Также исследовано влияние смещения проволок на амплитудные характеристики камеры.

Работа выполнена в Лаборатории ядерных проблем им. В.П.Джелепова ОИЯИ.

Препринт Объединенного института ядерных исследований. Дубна, 2001

Petrus A.Yu., Zalikhanov B.Zh. E13-2001-113
Electro-Mechanical Properties
of Narrow-Gap Multiwire Proportional Chambers

Electro-mechanical properties of narrow-gap proportional chambers are considered. An equation is obtained which allows evaluation of the working limits of such chambers in respect to high voltage depending on their geometrical characteristics. The influence of a wire shift on the chamber amplitude characteristics is investigated.

The investigation has been performed at the Dzhelepov Laboratory of Nuclear Problems, JINR.

Preprint of the Joint Institute for Nuclear Research. Dubna, 2001

Макет Т.Е.Попеко

Подписано в печать 05.07.2001
Формат 60 × 90/16. Офсетная печать. Уч.-изд. л. 2,07
Тираж 315. Заказ 52761. Цена 2 р. 50 к.

Издательский отдел Объединенного института ядерных исследований
Дубна Московской области